Computer Simulations of Nanoparticle Sintering

V. N. Koparde[*] and P. T. Cummings[**]

[*]Vanderbilt University, Nashville, TN, vishal.koparde@vanderbilt.edu
[**]Vanderbilt University, Nashville, TN, peter.cummings@vanderbilt.edu

ABSTRACT

During the vapor-phase synthesis of titanium dioxide (TiO_2) nanoparticles, sintering of the nanoparticles is an important aspect of their behavior and an understanding of this phenomenon is therefore important. In this work, molecular dynamics (MD) simulations of the coalescence of TiO_2 nanoparticles have been carried out. The driving force for sintering of nanoparticles is the reduction in potential energy due to the decrease in surface area. The loss of potential energy manifests itself as an increase in the temperature of the sintering particles. This work concentrates on 3 and 4nm anatase and rutile nanoparticles. Dependence of particle orientation on sintering is reported along with ion mobility studies in the core and neck regions.

Keywords: TiO_2, nanoparticles, sintering, molecular dynamics, simulation, anatase, rutile

1 INTRODUCTION

Nanoparticles have been the area of active research in recent years as they have novel and unique properties, which distinguish them from the bulk phase[1]. Considering the difficulties associated with experimental analysis at the nanoscale, these systems are good candidates for study using MD simulation. Titania nanoparticles are synthesized by oxidation of $TiCl_4$ in flame reactors at high temperatures and moderate-to-low pressures[2]. Nanoparticle sintering occurs in these reactors and is suitable for study at the molecular level. The stability between rutile and anatase has been reported to reverse with decrease in particle size[3]. So far, very few simulation studies have been reported on the coalescence of metal-oxide nanoparticles and their phase transformations. MD simulations will help to shed light on the fundamental transport mechanisms and the kinetics that govern the particle coagulation and to observe, at the atomistic level, any phase transformation.

Titania has three polymorphs found abundantly in nature, namely, anatase, rutile and brookite[4]. In bulk phase, anatase and brookite irreversibly and exothermally transform to rutile upon heating[5]. But at nanoscale, anatase is found to be the most stable phase[3]. In our studies, we concentrate on rutile and anatase, as they are the most important from applications point of view. Electronic and photocatalytic properties of these polymorphs tend to enhance considerably with decreasing particle size[3]. Recently, TiO_2 has been used as a photocatalyst for alcohol dehydration[6], in oxidation of aromatic compounds[7], degradation of paint pigments[8], removing contaminants from wastewater[9], and nitrogen oxide reduction[10].

Nanosized TiO_2 is manufactured by the "chloride" process[2], which involves vapor phase oxidation of $TiCl_4$ leading to the formation of amorphous nano-titania, which can then be annealed to the desired phase. The temperatures range from 973 to 1873K in this process[11]. During the thermal annealing following the chloride process, the titania nanoparticles collide with each other and sintering may occur to form larger particles. If the sintering time is less than collision time, then larger particles are produced; otherwise agglomerates are formed[12]. Various available sintering theories are not applicable to particles in the nanometer range as they cannot be treated as continuum elastic bodies but need to be subjected to more rigorous atomic treatment. In nanoparticles, the sintering mechanism is influenced by particle curvature and interatomic forces. Also, surface and grain boundary diffusion are found to be the most important transport processes in nanoparticle sintering. Some researchers also suggested that the high internal pressure of smaller particles could be responsible for the inapplicability of the available models to smaller particles. For example, the pressure inside a 10 nm TiO_2 particle is reported to be around 2000 atmospheres[13]. Such high internal pressures affect diffusion coefficients, which in turn affect the rates of particle sintering.

The impetus behind sintering of two TiO_2 nanoparticles is the decrease in the free energy due to a reduction in the surface area[14-16], which under the adiabatic environment causes a temperature rise. Formation of new chemical bonds may explain the rise in temperature. As solid-state diffusion, which is dependent on temperature, is the major transport mechanism in nanoparticle sintering, we can expect temperature to play a key role in process. Earlier studies found that the heat release due to particle coalescence may reduce the coalescence time by as much as a few orders of magnitude as in the case of silicon nanoparticles[16].

This work concentrates on the initial stages of TiO_2 sintering and the effect of phase, size and temperature on the sintering process. The systems under consideration contain two identical nanoparticles 3 or 4 nm in diameter. Rotating one of the particles in the system while keeping the other unchanged allows to look at the orientational dependence on sintering. The relative mobilities of ions in the neck and core regions of the sintering nanoparticles have also been reported.

2 SIMULATION DETAILS

A report[17] on the available force fields for TiO_2 suggests that the Matsui-Akaogi (MA)[18] is the most suitable for use in classical MD. This force field not only reproduces the structures of TiO_2 polymorphs but also outperforms more complex variable charge force fields. The MA force field describes the interaction between Ti and O ions as a sum of exponential-6 non-columbic terms and columbic interactions. It regards Ti and O ions to be rigid with +2.196 and -1.098 partial charges, respectively.

Spherical nanoparticles of the 3 or 4nm were cut out of larger anatase or rutile lattice[19]. Excess Ti or O ions were removed to obtain neutral particles. The sphere is duplicated and translated along x-axis to obtain a system containing two identical nanoparticles, which are separated by 1 nm. DLPOLY version 2.13[20,21] was used to carry out all the MD simulations with a timestep of 0.5 fs for a total time of 0.5 ns. The simulations were carried out in NVE ensemble in vacuum with no periodic boundary conditions, as this was the best way to imitate the low pressure conditions prevailing in the flame reactors. Simulations were repeated at different starting temperatures of 573, 973 and 1473K, which could be considered to represent the different temperature zones in the flame reactors.

3 RESULTS AND DISCUSSION

Snapshots of a typical TiO_2 nanoparticle sintering are shown in figure 1. The figure indicates that the particles are mutually attracting each other, before touching and forming a neck. It should be noted that no initial velocity is applied on the particles to induce collision. The non-elastic collision occurs in about 20-30 ps. The neck diameter gradually grows initially but then reaches a constant value.

The potential energy of the system drops as the nanoparticles come in contact as indicated in figure 2. But as the simulation is constant energy, the temperature simultaneously increases. For 3nm anatase or rutile particles the temperature rise is about 45K and for 4nm anatase or rutile particles it is about 30K. This rise is found to be independent of the initial temperature of the simulation as the amount of decrease in surface area is approximately identical in all cases, for a particular size.

To analyze the results in further detail a term called shrinkage is defined as follows,

$$shrinkage = \frac{\left(\frac{d_1 + d_2}{2}\right) - d_{COM}}{\left(\frac{d_1 + d_2}{2}\right)} \qquad (1)$$

where d_1 and d_2 are the diameters of the sintering nanoparticles while d_{COM} is the distance between their centers of mass at that instance.

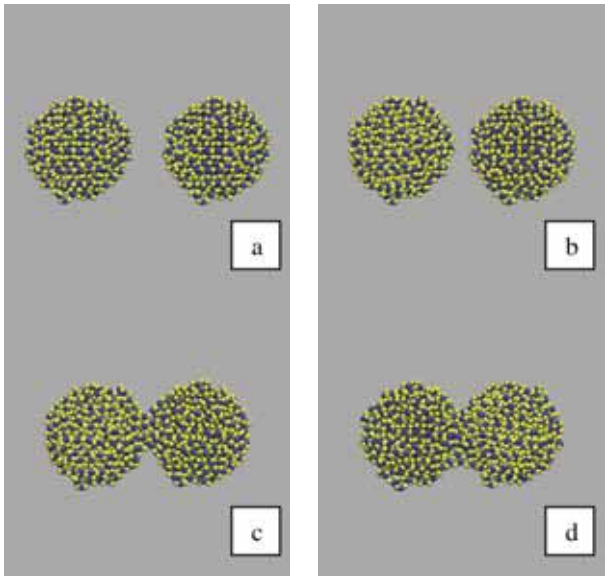

Figure 1. Snapshots of a typical sintering simulation

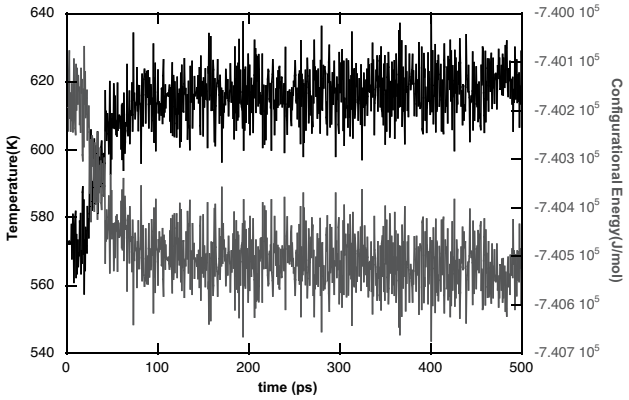

Figure 2. Time evolution of configurational energy and temperature of a typical sintering simulation (Two anatase 3nm particles with starting temperature of 573K)

Figure 3. shows the shrinkage variation with time for 3 and 4 nm anatase and rutile particle with a variety of different starting temperatures (mentioned in parenthesis). A negative shrinkage means that the particles are still separated while a positive shrinkage indicates particle interpenetration. Shrinkage seems to reach a constant value at the end of most of the simulations. This may be so because 0.5 ns is not long enough time to observe complete coagulation, which is reported to occur over a few microseconds[22]. If the simulations were run long enough, we would expect them to form a larger particle.

Neck diameter (not shown here) increased with temperature for 3nm anatase sintering particles but showed no such temperature dependence in case of 3nm rutile particles. For 3nm anatase case, it was ~17Å for a starting temperature of 573K while ~22Å for a starting temperature of 1473K.

Simulated x-ray diffraction patterns were calculated for the final agglomerates and they indicated no phase transformation over the time scale of the simulation. Examination of the neck regions explicitly showed that the neck region between two anatase particles was amorphous, while that between two rutile particles was rutile.

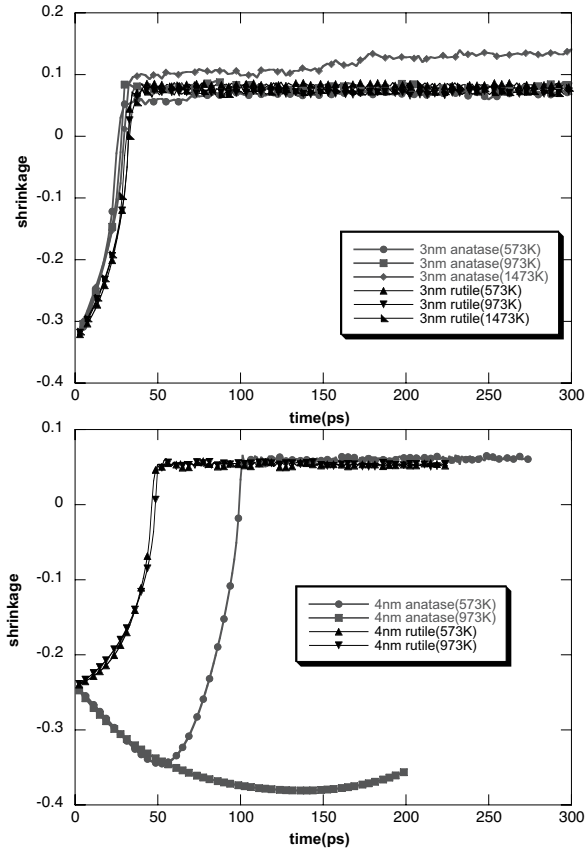

Figure 3. Shrinkage versus time for various simulations

3.1 Orientational Dependence

Crystallographic orientation is believed to play an important role in nanoparticle interaction. To study the effect of particle orientation the case of 3nm anatase sintering with the initial temperature of 573K was chosen and simulations were repeated after rotating the duplicated particle in the system through 20, 45, 90 and 180 degrees about z-axis at the beginning of the simulation. In all cases, except the 180-degree case, we observe neck formation. But in the 180-degree case the nanoparticles actually repel each other thus indicating that particle orientation is indeed important to the process of sintering. Also figure 4 shows that 90-degree orientation leads to maximum particle interpenetration. Such densification was experimentally observed and linked to anatase to rutile phase transformation[23] but the simulated x-ray diffraction patterns show no such phase transformation during the simulation.

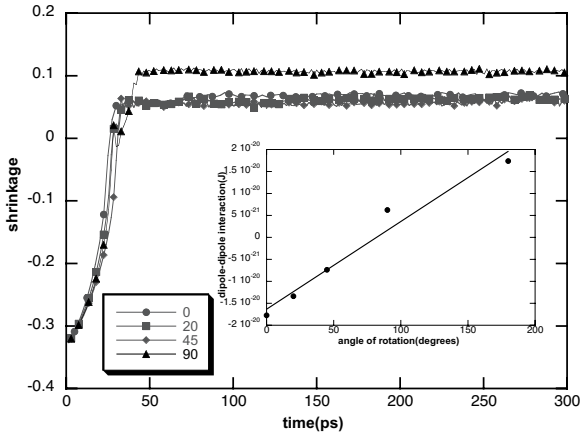

Figure 4. Dependence of orientation on sintering

To understand the orientational dependence in further detail, the dipole-dipole interactions between the nanoparticles at the beginning of the simulation were computed using the following formula[24],

$$W_{d-d} = \frac{\bar{\mu}_1.\bar{\mu}_2 - 3(\hat{n}.\bar{\mu}_1)(\hat{n}.\bar{\mu}_2)}{\left|\bar{r}_1 - \bar{r}_2\right|^3} \qquad (2)$$

where $\bar{\mu}_1, \bar{\mu}_2$ are the dipole moments of the particles, $\bar{r}_1, \bar{r}_2$ position vectors of the particles and $\hat{n}$ is the unit vector along $\bar{r}_1 - \bar{r}_2$. The dipole-dipole interaction becomes more repulsive with increase in orientational angle as indicated in figure 4 and at 180 degrees it is repulsive enough for the particle to not undergo neck formation. In all other cases, dipole-dipole interaction becomes attractive gradually as the simulation proceeds until the particles form a neck. Hence, it may be possible to model TiO_2 nanoparticles as spheres with fluctuating dipoles, before they collide.

3.2 Relative Ionic Mobilities

For further investigation of the sintering process, the relative ionic mobilities in the neck and core regions were determined. The relative displacement of the i^{th} ion from time t to t' is[25],

$$\Delta r_i(t,t') = \left[\left(\left(r_i(t) - r_i(t')\right) - \frac{1}{m_{Ti}n'_{Ti} + m_O n'_O}\mathrm{X}\left(\sum_{j=1}^{n'_{Ti}} m_{Ti}\left(r_j(t) - r_j(t')\right) + \sum_{k=1}^{n'_O} m_O\left(r_k(t) - r_k(t')\right)\right)\right)^2\right]^{1/2} \qquad (3)$$

Figure 5 shows the relative mobilities of Ti ions in the neck and core regions for the various simulations performed. Relative mobilities in the neck region are at least an order of magnitude greater than the core mobilities. There is no observable dependence of the neck ion relative mobilities on particle size or phase or initial temperature. At lower

temperatures, core ion mobilities of anatase nanoparticles are measured to be lower than those of rutile nanoparticles.

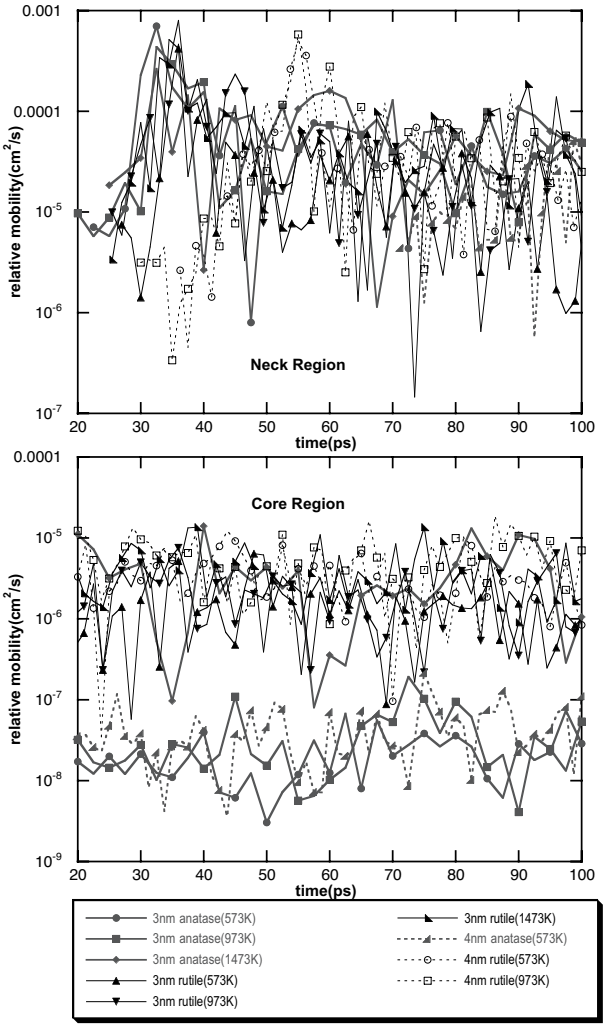

Figure 5. Relative Ti mobilities in neck and core regions

4 CONCLUSION

Initial stages of sintering of TiO_2 (anatase and rutile) nanoparticles have been studied using MD simulations. The sintering is very rapid and takes place in a few picoseconds. There is a temperature rise upon neck formation owing to the decrease in surface area. The temperature rise decreases with particle size but is independent of phase and initial temperature. Initial particle orientation is an important factor in nanoparticle sintering and its influence can be accounted for by considering the dipole-dipole interactions between the particles. Ions in the neck region are more mobile than those in the core. More simulations to study orientational dependence at higher temperatures are planned for the future. Further efforts will be made to correlate the simulation results and develop scaling laws for nanoscale sintering.

REFERENCES

[1] X.Z. Ding, X.H. Liu, Journal of Alloys and Compounds, 248, 143-145, 1997.

[2] M.K. Akhtar, X.O. Yun, S.E. Pratsinis, Aiche Journal, 37, 1561-1570, 1991.

[3] H. Zhang, J.F. Banfield, Journal of Materials Chemistry, 8, 2073-2076, 1998.

[4] C.M. Freeman, J.M. Newsam, S.W. Levine, C.R.A. Catlow, Journal of Materials Chemistry, 3, 531, 1993.

[5] M.M. Wu, J.B. Long, A.H. Huang, Y.J. Luo, S.H. Feng, R.R. Xu, Langmuir, 15, 8822-8825, 1999.

[6] M.A. Fox, M.T. Dulay, Chemical Reviews, 93, 341-57, 1993.

[7] M. Fujihira, Y. Satoh, T. Osa, Nature, 293, 206, 1981.

[8] P.A.M. Hotsenpiller, J.D. Bolt, W.E. Farneth, J.B. Lowekamp, G.S. Rohrer, Journal of Physical Chemistry B, 102, 3216-26, 1998.

[9] S.T. Martin, A.T. Lee, M.R. Hoffmann, Environmental Science & Technology, 29, 2567-2573, 1995.

[10] F. Gruy, M. Pijolat, Journal of American Ceramic Society, 75, 657, 1992.

[11] H.D. Jang, J. Jeong, Aerosol Science and Technology, 23, 553-560, 1995.

[12] M.R. Zachariah, M.J. Carrier, Journal of Aerosol Science, 30, 1139-1151, 1999.

[13] S.H. Ehrman, S.K. Friedlander, M.R. Zachariah, Journal of Aerosol Science, 29, 687-706, 1998.

[14] J.G. Gay, B.J. Berne, Journal of Colloid and Interface Science, 109, 90-100, 1986.

[15] K.E.J. Lehtinen, M.R. Zachariah, Physical Review B, 6320, art. no.-205402, 2001.

[16] K.E.J. Lehtinen, M.R. Zachariah, Journal of Aerosol Science, 33, 357-368, 2002.

[17] D.R. Collins, W. Smith, Council for the Central Laboratory of Research Councils, Daresbury, Research Report DL-TR-96-001, 1996.

[18] M. Matsui, M. Akaogi, Molecular Simulation, 6, 239-244, 1991.

[19] S.C. Abrahams, J.L. Bernstein, The Journal of Chemical Physics, 55, 3206-3211, 1971.

[20] W. Smith, Journal of Molecular Graphics, 5, 71-4, 1987.

[21] W. Smith, T.R. Forester, Journal of Molecular Graphics, 14, 136-41, 1996.

[22] A. Kobata, K. Kusakabe, S. Morooka, Aiche Journal, 37, 347-359, 1991.

[23] X.Z. Ding, X.H. Liu, Journal of Materials Research, 13, 2556, 1998.

[24] J.D. Jackson, Classical Electrodynamics, John Wiley & Sons Inc., 1975.

[25] H.L. Zhu, R.S. Averback, Philosophical Magazine Letters, 73, 27, 1996.